ELSEVIER

Polymer 42 (2001) 9413–9422

polymer

www.elsevier.com/locate/polymer

Structure property relationships in linear and cross-linked poly(imidonorbornenes) prepared using ring opening metathesis polymerisation (ROMP)

P.J. Hine[a], T. Leejarkpai[b], E. Khosravi[b], R.A. Duckett[a], W.J. Feast[b,*]

[a]*IRC in Polymer Science and Technology, University of Leeds, Leeds, LS2 9JT, UK*
[b]*Interdisciplinary Research Center in Polymer Science and Technology, University of Durham, South Road, Durham, DH1 3LE, UK*

Received 29 April 2001; accepted 2 July 2001

Abstract

The production and properties of a new family of materials synthesised via ring opening metathesis polymerisation (ROMP) is described. The monomers offer potential alternatives to dicyclopentadiene (DCPD) for either reaction injection moulding (RIM) or resin transfer moulding (RTM) use and provide new materials with an extended range of properties vis-à-vis poly(DCPD). Improvements include lower monomer odour together with control of both the reaction rate and the crosslinking reaction. A series of monofunctional imidonorbornene monomers, with different *N*-alkyl side chains, were polymerised to give a range of linear polymers, and, by copolymerisation with difunctional monomers with different *N*,*N*′-alkylene spacer lengths, a range of crosslinked materials. Processing conditions were established which gave over 95% conversion of the monomer for the linear materials, and over 95% gel fraction for the crosslinked materials. For the crosslinked materials, a value of the monomer:initiator ratio was established which gave homogeneously cured materials. The glass transition temperature (T_g) of the linear polymers was found to depend on the length of the alkyl side chain, while a sub T_g, β relaxation was observed, the position of which was independent of the side chain length. For the crosslinked polymers, the molecular weight between crosslinks was found to be lower than expected at low percentage loading of the crosslinking unit, and this was attributed to the contribution of physical crosslinks. At higher percentage loading of the crosslinking unit, the molecular weight between crosslinks was higher than expected, suggesting that under these conditions not all the crosslinking units were fully bound into the network, i.e. bound at both ends. Mechanical properties of the various materials were measured using the three-point bend geometry. Of particular interest were the high values of yield strength and toughness of the crosslinked polymers, which are comparable to known 'high toughness' materials, such as polycarbonate.

Keywords: Resin transfer moulding; Tough well-defined networks; ROMP

1. Introduction

A major motivation for this study was a desire to develop alternative monomers to dicyclopentadiene (DCPD) for reaction injection moulding (RIM) and resin transfer moulding (RTM) applications. DCPD, although a relatively cheap and commercially available material with important applications, suffers from a number of drawbacks. The advantages of DCPD include a rapid reaction, which is good for RIM and RTM applications, and good product mechanical properties including low density, low water absorption and excellent toughness. The disadvantages include a nauseating monomer odour, a strongly exothermic reaction, which proved difficult to control initially, uncertainty about the nature of the crosslinking reaction and difficulty in regulating it. Nevertheless, poly(DCPD) is a very interesting material which is finding market applications, as is evident from the number of published papers and patents which describe how DCPD can be used in commercial RIM systems [1–11].

The first aim of this current study was to synthesise alternatives to poly(DCPD) using ring opening metathesis polymerisation (ROMP) methodology [12–15] taking advantage of recent developments in catalyst stability [16–19]. Substituted norbornenes were chosen as the monomers for ROMP for a number of reasons. Firstly, they can be synthesised from cheap and readily available reagents; namely, cyclopentadiene, maleic anhydride, alkyl amines and α,ω-alkylenediamines and they have relatively low odour. Secondly, the final product can be made from the

* Corresponding author. Tel.: +44-191-374-3105; fax: +44-191-374-4651.
E-mail address: w.j.feast@durham.ac.uk (W.J. Feast).

0032-3861/01/$ - see front matter
PII: S0032-3861(01)00488-8

monomers without using a solvent. Thirdly, a wide range of material properties is possible, due to the combination of mono and difunctional monomers with different molecular and network structures. Fourthly, the final polymers can be linear (with good processability) or crosslinked (with better high temperature stability). A crucial factor in the development of the synthesis route was the availability of the ruthenium initiator developed by Grubbs et al. [16–19]. The advantages of this initiator over others include its stability towards functional groups and water, the possibility of well-controlled living polymerisation and its solubility in the monomers. Monofunctional *N*-alkyldicarboxyimidonorbornenes were synthesised and then polymerised in bulk in a mould to give linear polymers, and difunctional bis(*N*-alkylenedicarboxyimidonorbornenes) were synthesised for copolymerisation with the monofunctional monomers to produce crosslinked polymers.

A range of techniques was used to characterise both linear and crosslinked polymers in order to establish the optimum processing conditions for the synthesis of each type of product. Solution nuclear magnetic resonance (NMR) and differential scanning calorimetry (DSC) were used to follow the ROMP reaction of the monofunctional norbornenes [20,21]. Particular attention was given to maximising monomer conversion, as unreacted monomer can have a deleterious effect on thermal and mechanical properties. Having established appropriate conditions, samples were made using monomers with different alkyl side chain lengths. Dynamic mechanical thermal analysis (DMTA) was then employed to examine the variation in the relaxation behaviour, particularly the glass transition temperature T_g, with side chain length.

Solution NMR and DSC could not be used for the crosslinked materials, so DMTA proved the only useful way of establishing the optimum processing conditions and investigating the effects of molecular architecture (for example, the side chain and crosslink spacer lengths) on mechanical properties. Particular attention was given to measurements of the shear modulus above the glass transition temperature. This was used to determine a value for the molecular weight between crosslinks, using simple rubber elasticity theory and the results were compared to those expected from the stoichiometry of the monomer mixture.

2. Experimental

2.1. Mechanical property measurement

2.1.1. Dynamic mechanical thermal analysis (DMTA)

The major use of DMTA in this study was to help establish the optimum synthesis routes for the crosslinked polymers. Infrared analysis is often used to follow the cure of a thermosetting system, by looking at the change in an absorption peak characteristic of the crosslinking reaction. A typical example would be the fall in the contribution of the epoxide ring, as the crosslinking reaction of an epoxy resin proceeds. However, for the system in this study, there is no characteristic absorption line, which will differentiate between ring opening in the main chain, or as part of the crosslinking reaction. Therefore, there is no spectroscopic technique for following cure, and in the absence of a measurable T_g for the crosslinked polymers, DMTA analysis offered a way of assessing the extent of cure for the various combinations of reagents investigated.

When an amorphous glassy polymer passes through its glass transition, the modulus generally falls by about three orders of magnitude, from ~1 GPa below to ~1 MPa above T_g and this presents practical problems for mechanical testing. In this work, we have combined two different testing techniques to determine the dynamic behaviour on either side of the glass transition. Dynamic bend measurements were used to measure the behaviour below T_g, including the determination of the room temperature flexural modulus and the determination of any sub T_g, β relaxations. Dynamic torsion measurements were used to determine the glass transition temperature (T_g), the breadth of the glass transition and the shear modulus above T_g.

The majority of measurements, for temperatures at T_g and above, were made using a Rheometrics RDS II shear rheometer. The testing fixtures used were 8 mm diameter parallel plates, and the samples were 8 mm discs, approximately 5 mm thick. Tests were carried out over a range of temperatures using a ramp rate of 2°C min^{-1}, a dynamic strain of 0.5% and a test frequency of 1 Hz.

There were two problems with the dynamic torsion test, which arise as a consequence of the technique being developed for testing soft linear polymers, rather than entangled linear or crosslinked polymers below their T_g. The first problem was to obtain adequate bonding between the parallel plates and the polymer samples. The plates were lightly grit blasted to improve stress transfer. It also proved helpful to heat the polymer above its T_g prior to a run, in order to soften it and improve adhesion, and then carry out the temperature ramp test using a decreasing temperature protocol. For example, for testing a typical crosslinked polymer, the sample was first placed into the rheometer and a small compressive force was applied. The temperature was then raised to T_g + 20°C and held for 5 min to allow the sample to soften and adhere before the temperature was raised to T_g + 50°C. The test was then started the measurements being made as the sample was cooled to T_g − 20°C at 2°C min^{-1}. This technique proved most successful for the crosslinked polymers, due to their better high temperature stability. For the linear thermoplastics, the temperature was raised above T_g to adhere the samples to the plates, then lowered to below the T_g and the test was performed in an increasing temperature mode, again at a ramp rate of 2°C min^{-1}.

The second problem with the dynamic torsion test arose when measurements were made below T_g. It was found that as the modulus of the samples rose above 100 MPa, the

applied strain began to drop below the commanded strain of 0.5%, due to limitations of the instrument strain control. Measurements were recorded until the applied strain dropped to 80% of the command strain, this point defined the lowest test temperature that could be achieved for each material in torsion.

A second test instrument, a Rheometrics RSAII solids analyser, was used to measure the dynamic behaviour below and up to the T_g. The test geometry used for these tests was the clamped double cantilever beam. The sample (50 mm long, 5 mm wide and ~1 mm thick) was clamped at both ends and its centre: the central clamp was oscillated. The tests were carried out at a frequency of 1 Hz, using a dynamic strain of 0.2%, and a temperature ramp rate of 2°C min^{-1}. In this geometry, the mean strain was maintained at zero.

Fig. 1 shows typical data for Young's modulus, E, versus temperature for a linear thermoplastic (polyC6M see later) obtained from the two dynamic tests. The data from −100°C to +62°C were obtained from the three point bend geometry (Young's modulus E) and the data from +60°C to +150°C were obtained from the parallel plate shear geometry (shear modulus G). For the shear tests, a Young's modulus was calculated from the usual relationship $G = E/(2(1 + \nu))$, assuming a Poisson's ratio of 0.5, which is appropriate for a rubbery material above its T_g. The results shown in Fig. 1 demonstrate that the two sets of data superpose at temperatures where they overlap.

2.1.2. Static properties

The physical properties of the synthesised linear and crosslinked polymers at room temperature were also measured using a three-point bend test geometry. The test sample used was 5 mm wide, 3 mm thick and 25 mm long and the testing span was 20 mm. Tests were carried out on an RDP servo mechanical test machine, at a nominal strain rate of $10^{-3}\,s^{-1}$. Flexural strength was measured using unnotched samples. If the sample was found to yield, the yield stress was taken as the point of onset of nonlinearity.

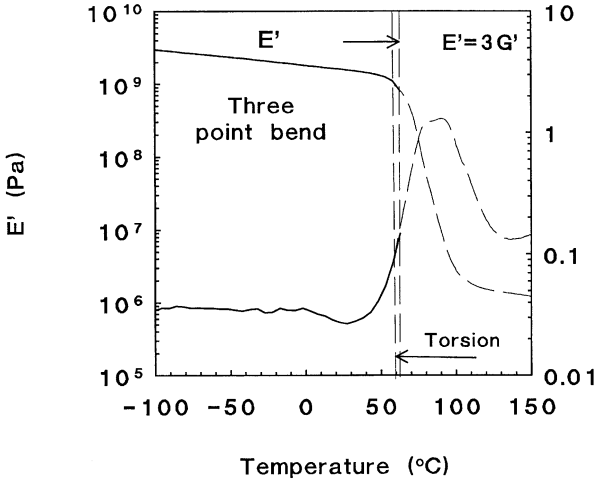

Fig. 1. Young's modulus, E, and tanδ, for the linear polymer (polyC6M), for the three-point bend geometry and the torsion shear geometry.

The fracture properties of a number of the crosslinked polymers were also measured using the three point bend geometry and similar sized samples. In order to obtain linear elastic fracture mechanics parameters, a crack was introduced at the centre of the sample using a saw, which was then sharpened by tapping a razor blade into it. A crack length (a) to width (W) ratio of between 0.45 and 0.55 was the target, as specified in the ESIS fracture testing standards [22]. The geometry independent fracture toughness parameter K_c, the critical stress intensity factor, was then calculated from

$$K_c = \frac{PY}{BW^{1/2}} \quad (1)$$

where P is the fracture load, B the sample thickness and W the sample width. Y is a geometry dependent parameter, given as a function of (a/W) in Ref. [22]. The critical strain energy release rate, G_c, was then calculated from the usual relationship

$$K_c^2 = EG_c \quad (2)$$

2.2. Gel fraction

The gel fraction of the crosslinked polymers was determined by extraction with boiling chloroform for three days, followed by drying in an oven for one day at 60°C. The gel fraction (percent) was determined as a ratio of the final weight after extraction and drying, W_{final}, divided by the initial weight, $W_{initial}$.

$$\text{Gel fraction} = \frac{W_{final}}{W_{final}} \times 100 \quad (3)$$

2.3. Differential scanning calorimetry (DSC)

DSC experiments were carried using a Perkin–Elmer DSC7 (indium calibration), to determine the glass transition temperature of the linear polymers. Scans were carried out at a ramp rate of 10°C min^{-1}.

3. Results and discussion

3.1. Establishing the optimum synthesis routes for the linear and crosslinked polymers

The synthesis of the mono and difunctional monomers has been described previously [13,14,20,21]. Two types of monomers were used, both based on *N*-alkyl norbornene dicarboxyimide. The first, termed *monofunctional*, *N*-alkyl-dicarboxyimidonorbornenes carrying pendant alkyl chains of different lengths (Fig. 2a). The monomer was synthesised in both endo and exo forms: the exo isomers were preferred because, although the product polymers had lower T_g

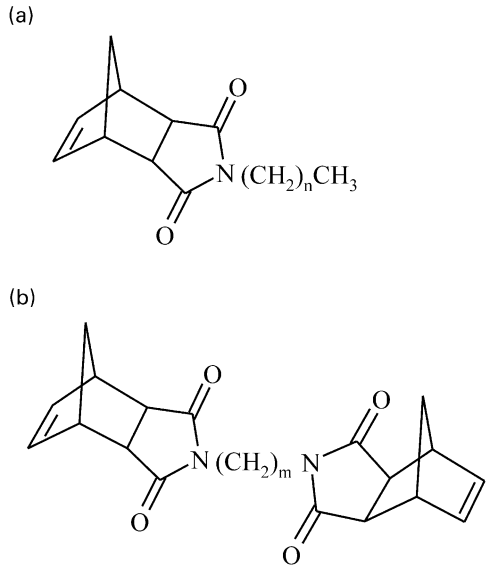

Fig. 2. The chemical structures of the (a) monofunctional monomer *N*-alkyldicarboxyimidonorbornenes and (b) the difunctional monomer bis(*N*,*N*′-alkylenedicarboxyimidonorbornenes).

values, the exo monomers were much more reactive than their endo analogues. The monofunctional monomers synthesised, termed C*n*M, included $n = 3, 4$ and 5. The second type of monomers synthesised for this study were *difunctional* bis(*N*,*N*′-alkylenedicarboxyimidonorbornenes) with an alkylene spacer (Fig. 2b). These materials, termed C*m*D, were synthesised for values of $m = 3, 5, 6, 9$, and 12.

The C*n*M monomers were polymerised using the Grubbs' ruthenium initiator, $Cl_2Ru(=CHPh)((PC_6H_{11})_3)_2$. In the first series of experiments, using the C6M monomer, the initiator was mixed with the monomer (monomer:initiator 4000:1) at room temperature and stirred for 10 min. The reaction mixture was transferred into a mould (two glass blocks separated by a silicone rubber gasket) which was placed in an oven set at 160°C for 1 h. Only 80% monomer conversion (measured using solution NMR) [21]was achieved under these conditions: the resultant polymer had a T_g of 35°C. In the second set of experiments, the mould was first kept in an oven set at 60°C for 20 min and then the temperature was raised to 160°C for 1 h. The additional time at the intermediate temperature of 60°C, gave a 98% conversion with a maximum T_g of ~80°C. The importance of obtaining a high monomer conversion is indicated by the results shown in Fig. 3, where the percentage degree of monomer conversion is plotted against the glass transition, T_g, of the resulting material (determined from DSC) for various samples. The figure confirms the monomer as a very efficient plasticiser of the polymer, and that high degrees of conversion are required in order to obtain a high T_g.

The protocol adopted in this work for processing C6M was: (1) the initiator was mixed with the monomer at 20°C for 15 min; (2) the mixture was transferred to the mould; (3) the temperature was raised to 60°C and the mixture was left for 20 min; (4) the mixture was heated to 160°C for 60 min;

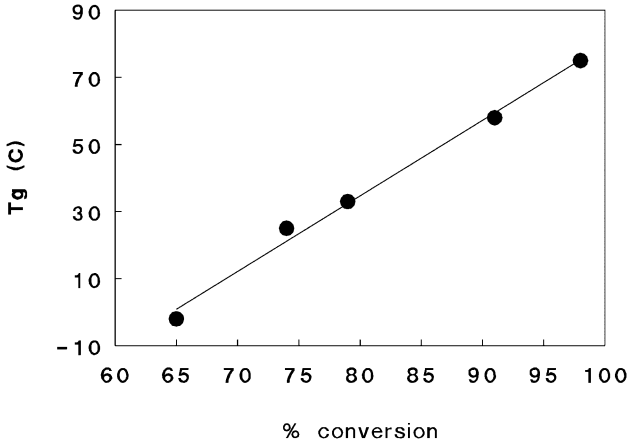

Fig. 3. Glass transition temperature, T_g, versus the % of monomer conversion for polymerisation of C6M.

(5) the oven was set to room temperature and force cooled (ca 2 h) and the polymer removed from the mould. The monomer:initiator ratio used at this stage was 4000:1. A similar procedure was established for the C5M monomer. For the C4M monomer, the mixing temperature had to be raised to 35°C, while for the C3M monomer the mixing temperature had to be raised even further to 50°C. While C4M was successfully polymerised, the elevated temperature needed to melt the C3M monomer had the effect of increasing the rate of polymerisation with the consequence that gelation occurred very early and high monomer conversion in this bulk polymerisation was never obtained.

Crosslinked polymers were formed by co-polymerising the difunctional and the monofunctional monomers in the presence of the ruthenium initiator. The procedure, as developed first for a combination of the C5M monomer and 2 M% of the C12D difunctional monomer, was as follows. First, the difunctional monomer was dissolved in the monofunctional monomer, and then the initiator was added. This mixture was stirred at 20°C until just before gelation, at which point the mixture was transferred to the mould. To determine the gelation point, a sacrificial sample was stirred until gelation occurred. Once in the mould the sample was left for an hour for the reaction to go to completion. Initial tests used conditions similar to those established for the synthesis of the linear polymers, that is a curing temperature of 160°C and a monomer:initiator ratio of 4000:1. Gel fraction measurements, obtained by extraction of the resultant crosslinked materials with chloroform for three days at 60°C, showed that samples cured at 160°C had a low gel fraction, probably as a result of the reaction proceeding too quickly. Lowering the cure temperature to 100°C increased the gel fraction to around 80%, although the samples were still inhomogeneous in terms of their relaxation behaviour, suggesting an uneven cure.

A further series of experiments was carried out varying the monomer:initiator (*M*:*I*) ratio and using the lower cure temperature of 100°C samples were made for *M*:*I* of 4000:1,

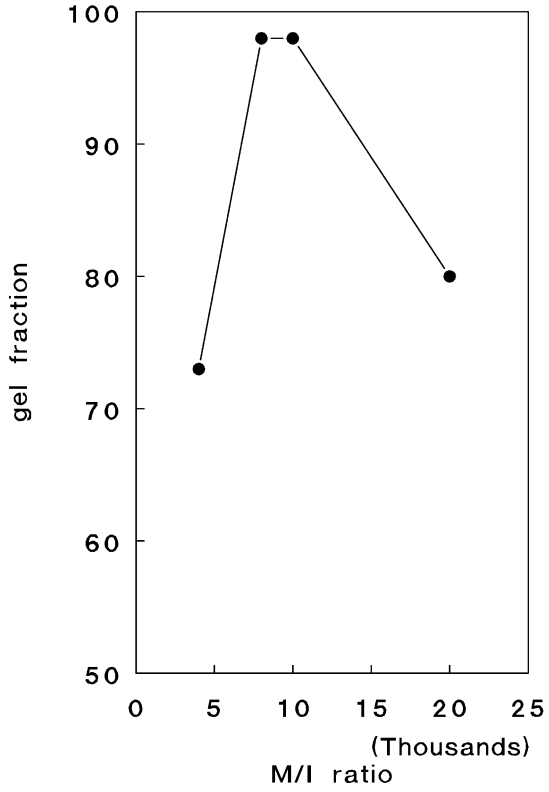

Fig. 4. Gel fraction versus *M*:*I* ratio for C5M polymerised with 2 M% of C12D.

8000:1, 10,000:1 and 20,000:1. Although a similar mixing time, i.e. the time to gelation, was established for the 8000:1 *M*:*I* ratio, the mixing time had to be increased to 40 min for a ratio of 10,000:1 and to 60 min for 20,000:1. Fig. 4 shows gel fractions for this series of samples. It is seen that, for these monomers with this initiator combination, the highest gel fractions, ~97%, are obtained for an *M*:*I* ratio of 8000:1–10,000:1.

Figs. 5 and 6 show dynamic torsion mechanical results for a series of C5M + 2%C*m*D crosslinked polymers made using these different *M*:*I* ratios. The 4000:1 ratio sample (Fig. 5) used the C5D difunctional monomer, while the other three samples (Fig. 6) used the C12D monomer. Results presented later (Figs. 14 and 15) show that the length of the alkylene chain in the difunctional link does not significantly affect the behaviour through the glass transition so we can safely use this series to assess the effect of the *M*:*I* ratio, even though the C*m*D component is different.

Fig. 5 shows results for *M*:*I* = 4000:1 (C5D) [curve a] and 8000:1 (C12D) [curve b], while Fig. 6 shows results for *M*:*I* = 8000:1, 10,000:1 and 20,000:1 (all C12D) [curves a,b and c respectively]. For the highest amount of initiator ($M : I = 4000 : 1$), which was the optimum ratio established for the synthesis of linear polymers, the results showed firstly a very broad transition and secondly no plateau shear modulus above T_g: both are a clear indication that a homogeneous fully crosslinked network had not been

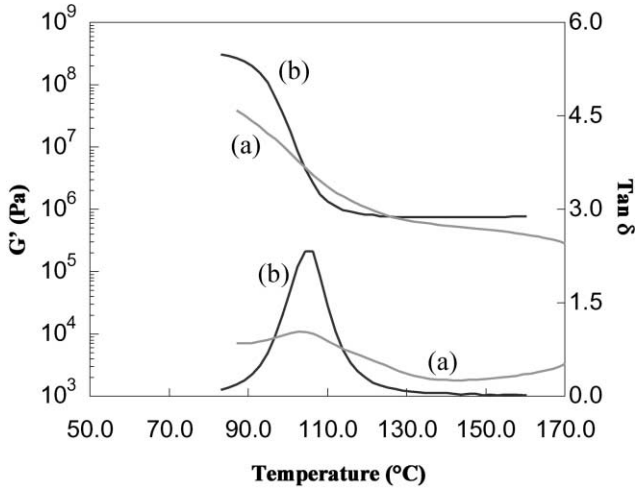

Fig. 5. Shear modulus G' and tanδ versus temperature for C5M polymerised with 2 M% of C*m*D: *M*:*I* = (a) 4000:1 (C5D) and (b) 8000:1 (C12D).

developed during curing. This is not unexpected considering the gel fraction results shown in Fig. 4. For an *M*:*I* ratio of 8000:1, a much sharper transition was observed, accompanied by a plateau modulus above T_g, both indications of a highly developed crosslinked network. For an *M*:*I* ratio of 8000:1, the time to gelation (or the time after which the mixture could not be transferred to the mould) had not increased over that for a ratio of 4000:1. As the *M*:*I* ratio was increased further (Fig. 6), the transition became broader again, accompanied by a reduction in the plateau shear modulus above T_g, which is an indication of a reduction in the crosslink density. These results, taken together with the gel fraction results shown in Fig. 4, indicate that for the C5M/C*m*D combinations, an *M*:*I* ratio of 8000:1 is near optimum in terms of developing a homogeneously cured network: whether it is optimum in terms of the total reaction

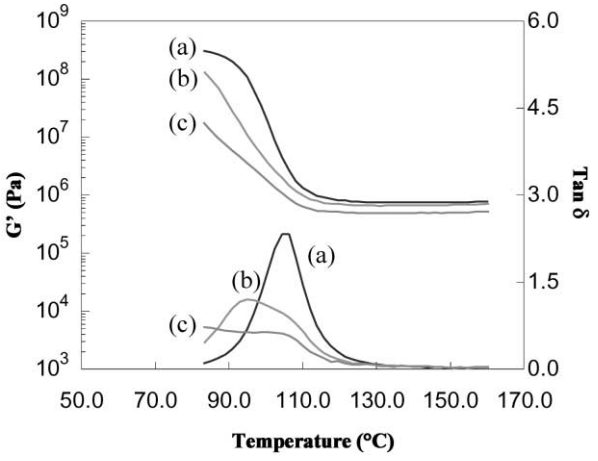

Fig. 6. Shear modulus G' and tanδ versus temperature for C5M polymerised with 2 M% of C12D: *M*:*I* = (a) 8000:1 (b) 10000:1 and (c) 20000:1.

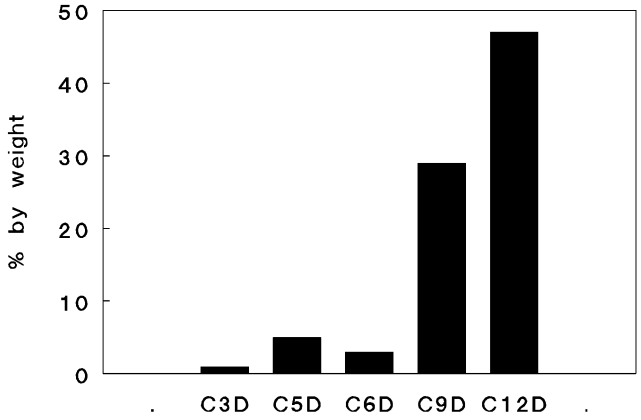

Fig. 7. The solubility of C*m*D difunctional monomers in the C5D monofunctional monomer.

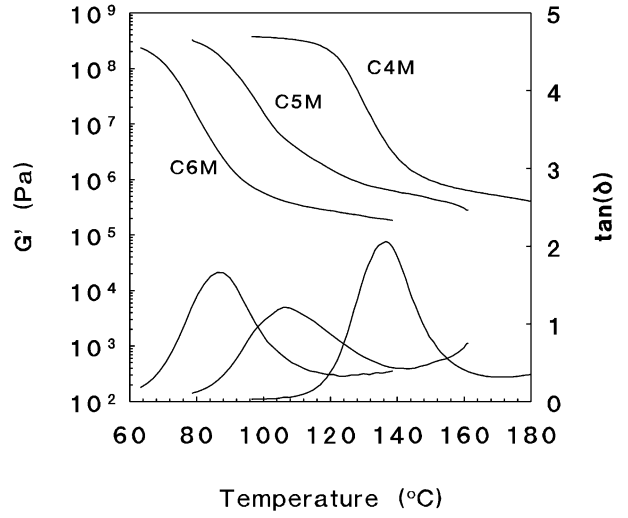

Fig. 8. Torsion modulus G' and tanδ versus temperature for polyC4M, polyC5M and polyC6M.

time, which might be most relevant for an industrial process, is of course a different question.

A key issue for synthesis of the crosslinked materials is the solubility of the difunctional monomers in the monofunctional monomers, as this controls the possible combinations that are available. Fig. 7 shows a set of maximum solubilities for a range of the C*m*D difunctional monomers in the C6M monofunctional monomer. Solubilities were measured by dissolving small amounts of the C*m*D difunctional monomers in the C6M monomer until the limit was found. It is seen that there is an increase in the maximum solubility as the spacer length increases, apart from the C6D monomer, which shows contrary behaviour. This general increase in solubility with increasing spacer length was also seen when dissolving the C*m*D in the C4M and C5M monomers.

Having established the optimum processing conditions, for both the linear and crosslinked polymers, the mechanical behaviour of samples made under these conditions was investigated.

3.2. Mechanical properties — linear polymers — CnM

Fig. 8 shows a comparison of the dynamic torsion results (measured at a frequency of 1 Hz) for polyC*n*M materials with $n = 4$, 5 and 6. It can be seen that the shape of the curves is very similar, but that the glass transition temperature, T_g, falls with increasing alkyl side chain length (in all the following discussions, the glass transition temperature is taken as the peak in tanδ). If the shear modulus results are plotted against $(T - T_g)$, rather than the temperature, T, the curves superimpose and have a very similar shape. The fall in T_g with side chain length has been seen before by workers investigating other systems, most notably by Hoff et al. in their work on alkyl methacrylates [23,24]. Fig. 9 shows the Hoff results in comparison with the current poly(imidonorbornene) results. There is a clear correspondence between the effect of the side chain length on T_g between the two systems, apart from an offset, which is presumably due to differences in the main chain stiffness. The reason for the variation in T_g with side chain length proposed by Hoff is that the longer side chains cause a reduction in T_g by mediation of interchain forces via internal plasticisation.

Measurements were also made of the sub T_g behaviour of the polyC*n*M thermoplastics using dynamic three point bend tests. Results showed a very broad sub T_g, β relaxation centred around −100°C, with the position independent of the side chain length. As the side chain length was increased, the height of the transition decreased such that for the polyC6M the peak was almost undetectable. The independence of the position of the β relaxation from the length of the side chain, mirrors the data published on methacrylate studies [24], where it was proposed that the β process is due to co-operative motion within the side chain and so does not depend on the side chain length above a minimum length. It has often been suggested that the position of the β relaxation for a polymer is associated with the brittle–ductile transition [25,26]. A β transition of −100°C could be very advantageous for it is possible that the material could show ductile, or at least 'pseudo-ductile' behaviour down to low temperatures.

However, the work of Wellinghoff and Baer [27], suggests that the correlation between a β relaxation and the brittle–ductile transition only exists when the secondary relaxation is due to main chain, rather than side chain, motion. Future work is planned to investigate possible links between the β relaxation and the brittle–ductile transition in these types of polymer.

Some preliminary physcial properties were measured for the polyC4M, polyC5M and polyC6M and the results are shown in Table 1. The polyC4M had the highest density of 1150 kg m^{-3}, with the other two polymers showing a similar density of 1100 kg m^{-3}. The room temperature modulus was found to fall with increasing side chain length, a consequence of the different temperature differences between

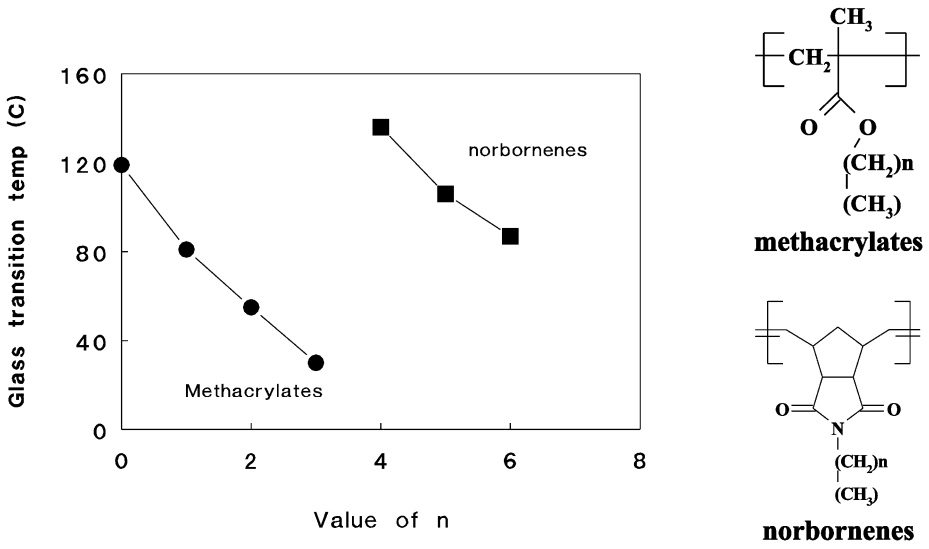

Fig. 9. Glass transition temperature, T_g, versus side chain length for the norbornene linear polymers in comparison with alkyl methacrylates.

room temperature (20°C) and T_g for the three polymers, as mentioned earlier. The yield stress (measured in the three point bend test) fell with increasing side chain length. A much more detailed study of the effect of the side chain length on deformation behaviour will form the basis of future studies.

3.3. Mechanical properties — crosslinked polymers — *CnM + x% CmD*

The results described above in Figs. 5 and 6 showed that the optimum *M:I* ratio for the C5M/C*m*D system was 8000:1. Having established this fact, a range of samples was prepared using this ratio, to investigate the effect of varying the percentage of the difunctional component, and the length of the difunctional linkage. Fig. 10 shows the dynamic shear modulus results for the C5M/C12D combination, with 1, 5 and 10 M% of the difunctional component. The results show that as the percentage of the difunctional, crosslinking unit, is increased the glass transition shifts to a higher temperature, the height of the tanδ peak decreases and the plateau shear modulus above T_g increases. These results are as expected for an increase in the crosslink density of a polymer. Nielsen [28] in his review of the crosslinking effect on the physical properties of polymers, describes these three effects. With regard to the shift in T_g, Nielsen reports that although a number of studies have been made in this area, the different studies do not agree very well. The amount that T_g shifts, due to the same fractional increase in crosslink density, is different for different systems, although it invariably increases. The reduction in the height of the tanδ peak is a direct result of the increase in the plateau shear modulus, as it is a reflection of the difference between the plateau values above and below the transition. It is worth noting that the results suggest that the modulus below T_g is independent of the degree of crosslinking, as expected.

The most interesting aspect of these dynamic torsion results is that they can be used to obtain a measure of the crosslink density of the synthesised polymers. Many authors, including Nielsen [28], have utilised the kinetic theory of rubber elasticity [29] to calculate the molecular weight between crosslinks, as above T_g a crosslinked polymer behaves substantially like a rubber. Rubber elasticity relates the shear modulus, G, to the molecular weight between crosslinks, M_c;

$$G = \frac{\Phi \rho RT}{M_c} \tag{4}$$

where ρ is the polymer density, R is the gas constant, T the absolute temperature and Φ is the front factor. There has been extensive discussion in the literature regarding the most appropriate value for the front factor Φ. While many authors set this equal to unity, others state it depends on the

Table 1
The mechanical properties of the C*n*M linear polymers

Polymer	T_g (°C)	T_β (°C)	Density (kg m^{-3})	Modulus (20°C) (GPa)	Yield strength (20°C) (MPa)
C4M	136	−99	1150	2.36	67.4 ± 5.7
C5M	106	−95/−105	1100	1.53	60.4 ± 2.1
C6M	87	Very broad	1100	1.46	42 ± 2.0

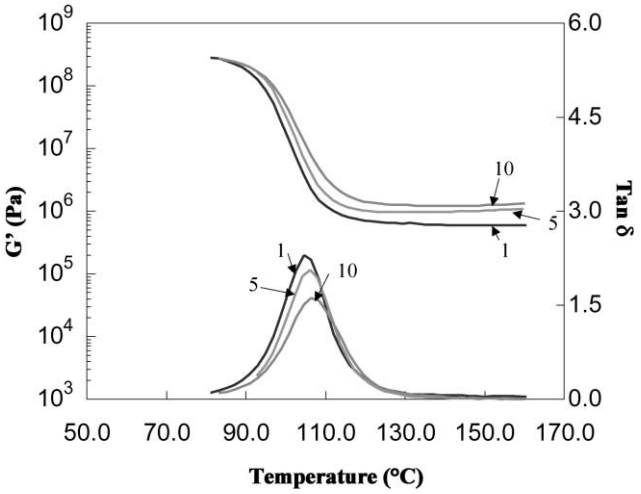

Fig. 10. Dynamic torsion results for C5M + x molar percent of C12D: x = 1, 5 and 10.

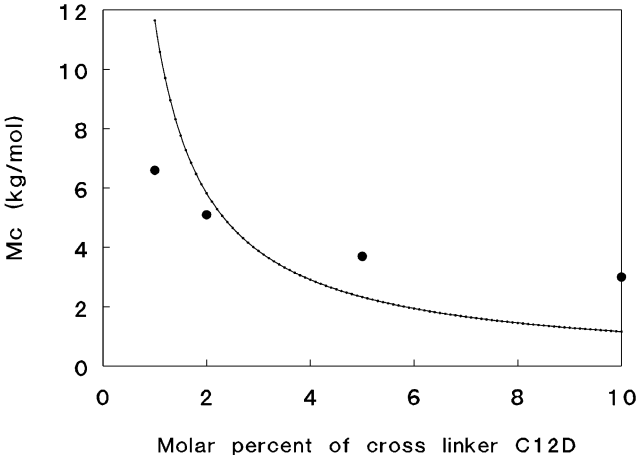

Fig. 11. A comparison of the theoretical molecular weight between crosslinks (solid line) with the calculated value (●), for the C5M/C12D polymer.

functionality of the crosslinking unit. Lesser [30] in particular, based on the work of Graessley [31], states that where the crosslinks are mobile $\Phi = (f-2)/f$, where f is the crosslink functionality, whereas in networks where the crosslink mobility is suppressed, $\Phi = 1$. Most authors agree that exact numerical agreement is not expected due to a number of effects, including non-Gaussian chain behaviour at high crosslink densities, network imperfections and physical or trapped entanglements. In this work, we have assumed the front factor to be equal to 1.

The above equation has been shown to hold fairly well as long as the measurements are carried out slowly (~1 Hz), at or close to equilibrium. Eq. (4) would suggest that above T_g, the shear modulus should rise as the temperature is increased. Although there is some suggestion from Fig. 10 that the result for the C5M/5%C12D polymer shows this effect, in general the crosslinked materials all showed a plateau modulus.

The arbitrary decision was taken to choose the shear modulus at 50°C above T_g, G_{T_g+50}, to determine the molecular weight between crosslinks. Eq. (2), in terms of M_c, then becomes

$$M_c = \frac{\rho R(T_g + 50)}{G_{T_g+50}} \tag{5}$$

It is of interest to compare the value of M_c determined in this way from the mechanical measurements, with that expected from the chemistry. It can be shown that the theoretical value of M_c^{Theory}, for a 100% perfect reaction, is given for this system by

$$M_c^{\text{Theory}} = \frac{\text{molecular weight of CnD monomer}}{\text{molar fraction of CmD monomer} \times 2} \tag{6}$$

Fig. 11 shows a comparison between the molecular weight between crosslinks calculated from Eq. (6) (theory) and from the measured shear modulus together with Eq. (5). The results, including the addition of a 2 M% sample, show that at low amounts of the crosslinker, the molecular weight between crosslinks is less than theory predicts, while for high amounts of the crosslinker the theory under predicts the molecular weight between crosslinks. Put another way, at low percentages of the crosslinker the crosslink density is higher than predicted by theory, while at higher percentages of crosslinker the crosslink density is lower than predicted.

At low crosslink densities, the molecular weight between crosslinks is more than the entanglement molecular weight, so that the shear modulus that is measured is due to a combination of chemical crosslinks and physical entanglements. Many authors have proposed that the total number of crosslinks is a sum of the chemical and physical crosslinks, so we can introduce a second term into Eq. (4) [32,33] giving

$$G = \frac{\rho RT}{M_c^{\text{total}}} = \rho RT\left(\frac{1}{M_e} + \frac{1}{M_c}\right) \tag{7}$$

where M_c is the molecular weight between the chemical crosslinks and M_e is the entanglement molecular weight. From the results in Fig. 11, this gives a M_e as ~15,000. This value is comparable with values reported for similar polymers. Fischer [34], for example, gives values of 2500, 9200 and 19,000–32,000 for polycarbonate, PMMA and polystyrene respectively, while Mark [35] gives comparable values of 10,000 for PMMA and 13000 for polystyrene. Such a value of M_e would predict a shear modulus of the uncrosslinked polymer of ~0.3 MPa, which is consistent with the results in Fig. 8. At high percentages of crosslinker, the crosslink density is less than expected. We propose that in this case, a proportion of the difunctional units are ineffective as crosslinkers, due to being connected to the network at only one end. There is at present, no available method (i.e. spectroscopic) for corroborating this important assumption. However, a similar comparison between theory and experiment has been seen before in work carried out in this department on crosslinked PMMA [36].

In the next series of experiments, the difunctional group was kept as C12D, but the monofunctional monomer was

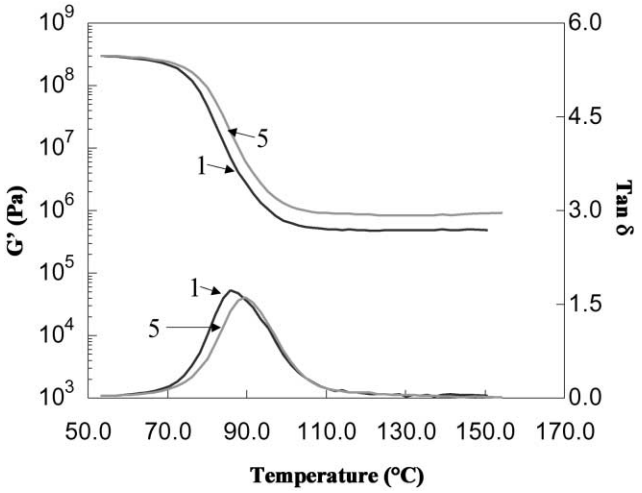

Fig. 12. Dynamic torsion results for C6M + x molar percent of C12D: x = 1 and 5.

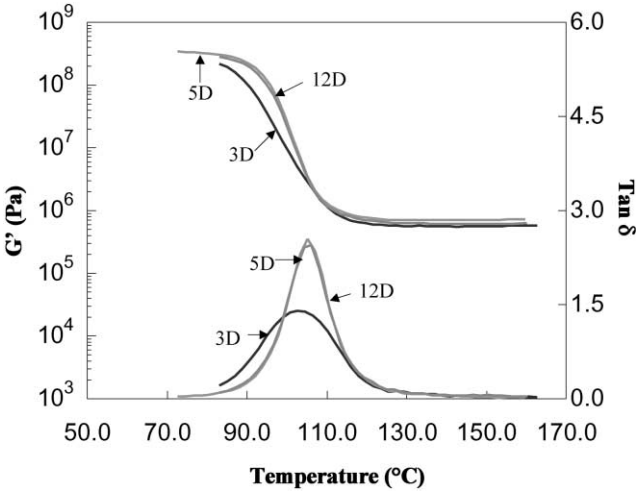

Fig. 14. Dynamic torsion results for the C5M + 2 M% of CmD: m = 3, 5 and 12.

changed to C6M. Polymerisation was via the same procedure established from the C5M/C12D system, using an M:I ratio of 8000:1. Fig. 12 shows the results of torsion tests on two of these polymers: 1 and 5 M% of C12D. The results are very similar to the C5M/C12D system apart from the lower T_g. The same features are again evident: a plateau modulus above T_g which increases with increasing molar percentage of crosslinker, and a sharp T_g, the position of which shifts up in temperature with increasing amount of crosslinker. Fig. 13 shows a comparison between the theoretical M_c and the experimentally determined M_c as for Fig. 11. The comparison is analogous to that for the C5M system. The difference in the results at 1% molar percentage is again attributed to the presence of physical entanglements: the entanglement molecular weight for this system, derived using Eq. (5), was ~20000.

Finally Figs. 14 and 15 show the effect of changing the length of the difunctional spacer on the behaviour around the glass transition, for a 2 molar percentage of the difunctional unit. Fig. 14 shows the dynamic torsion results for the C5M + 2 M% of a C3D, C5D and C12D difunctional unit: Fig. 15 shows the same measurements for the C6M + 2 M% of a C3D, C6D and C12D difunctional unit. In both cases, there is little difference between the C12D and the C5/6D units. In both cases, the polymers synthesised using the C3D difunctional monomer show a broader more inhomogeneous transition. This may be due to the different reactivity, and poor solubility of the crosslinker with the shorter spacer unit, but it could also be that the chosen M:I ratio of 8000:1 is not optimum for the shorter, more reactive, species. We can conclude that, as the length of the difunctional unit does not appear to affect the T_g and crosslink density at this molar percentage of the crosslink unit, it would be best to use the longest available (i.e. the C12D difunctional monomer) as this is the most soluble and can be used in higher percentages if required.

Finally, Table 2 summarises the measured mechanical

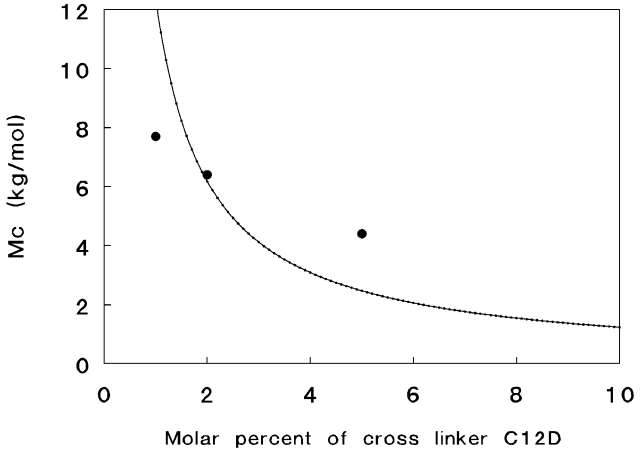

Fig. 13. A comparison of the theoretical molecular weight between crosslinks (solid line) with the calculated value (●), for the C6M/C12D polymer.

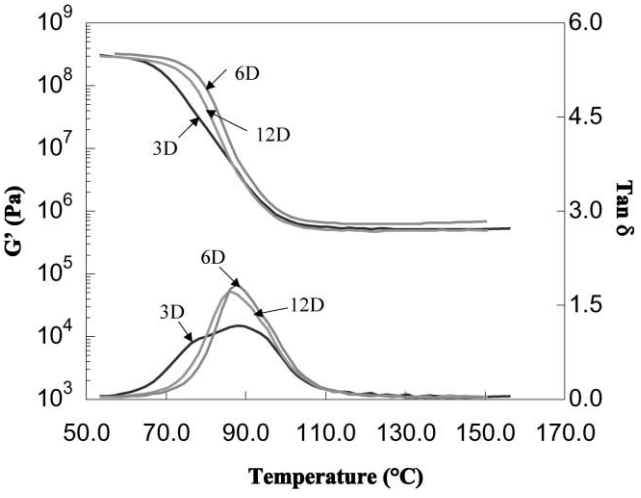

Fig. 15. Dynamic torsion results for the C6M + 2 M% of CmD: m = 3, 6 and 12.

Table 2
The mechanical properties of the crosslinked polymers

Polymer	T_g (°C)	Density (kg m^{-3})	Modulus (Gpa)	K_c (MNm $^{-3/2}$)	G_c (kJ/m^2)	Yield/fracture strength (MPa)
C4M/2%C12D	117	1136	2.7 ± 0.2	2.4 ± 0.2	2.2 ± 0.2	61 ± 15 (F)
C5M/2%C12D	105	1120	2.2 ± 0.2	2.8 ± 0.2	3.5 ± 0.6	72 ± 2 (Y)
C6M/2%C12D	87	1092	1.9 ± 0.1	2.6 ± 0.1	3.5 ± 0.2	59 ± 3 (Y)
Polycarbonate	150	1200	2.3	3	3.9	62 (Y)
Polystyrene	95	1050	3.1	1.1	0.4	45–55 (F)

properties for the C*n*M/2%C12D series of crosslinked materials. The room temperature flexural moduli and bending strength are, in general, higher than the equivalent thermoplastics (Table 1). Of particular interest are the high values of yield strength and toughness, which are comparable to known 'high toughness' materials, such as polycarbonate (Table 2). The C5M/2%C12D material shows the best combination of properties with a very high yield strength and excellent fracture toughness. We can conclude that this class of new polymers has very interesting mechanical properties and appears to open definite prospects for RTM when larger quantities of polymer become available.

4. Conclusions

The results presented above demonstrate that it is possible to design mixtures of mono and difunctional monomers which undergo efficient crosslinking in bulk in a mould under the influence of the Grubbs' ruthenium ROMP initiator. The product materials display an extended range of physical properties and the monomers are potentially cheap and are of low odour. Further sets of mono and difunctional monomers are being investigated in an attempt to extend the range of materials available via this approach.

Acknowledgements

We thank the Engineering and Physical Sciences Research Council for financial support, one of us (TL) thanks the Thai Government for a scholarship and we thank Alan M. Kenwright for help with NMR work.

References

[1] Minchak RJ. US Patent 4,426,502, issued 17/01/1984.
[2] Matejka L, Houtman C, Macosko CW. J Appl Polym Sci 1985;30:2787–803.
[3] Grubbs RH, Johnson LK, Nguyen ST. US Patent No. 5,312,940, issued 5/17/1994.
[4] Grubbs RH, Johnson LK, Nguyen ST. US Patent No. 5,342,909, issued 8/30/1994.
[5] Grubbs RH, Nguyen ST, Johnson LK. US Patent No. 5,710,298, issued 1/20/1998.
[6] Grubbs RH, Woodson Jr CS. US Patent No. 5,728,785, issued 3/17/1998.
[7] Woodson Jr CS, Grubbs RH. US Patent No. 5,939,504, issued 8/17/1999.
[8] Breslow DS. CHEMTECH 1990:540–4.
[9] Johnson JA, Farona MF. Polym Bull 1991;25:625–7.
[10] NG H, Manas-Zloczower I, Shmorhun M. Polym Engng Sci 1994;34:921–8.
[11] Bell A. Polym Prepr 1994;35:694–5.
[12] Feast WJ, Khosravi E. Recent development in ROMP. In: Ebdon JR, Eastmond GC, editors. New methods of polymer synthesis, vol. 2. London: Blackie Academic and Professional, 1995. Chapter 3.
[13] Khosravi E, Al-Hajaji AA. Polymer 1998;39:5619–25.
[14] Khosravi E, Al-Hajaji AA. Eur Polym J 1998;34:153–7.
[15] Grubbs RH, Khosravi E. ROMP and related processes. In: Schluter A-D, editor. Synthesis of polymers: a volume of materials science and technology. Wiley–VCH, 1998. p. 65–104, Chapter 3.
[16] Nguyen ST, Grubbs RH, Ziller JW. J Am Chem Soc 1993;115:9858–9.
[17] Hillmeyer M, Laredo WR, Grubbs RH. Macromolecules 1995;28:6311–6.
[18] Schwab PE, France MB, Ziller JW, Grubbs RH. Angew Chem Int Ed Engl 1995;4:2039–41.
[19] Schwab PE, Grubbs RH, Ziller JW. J Am Chem Soc 1996;118:100–10.
[20] Khosravi E, Feast WJ, Al-Hajaji AA, Leejarkpai T. J Mol Catal A: Chemical 2000;160:1–11.
[21] Leejarkpai T. PhD Thesis, University of Durham, UK, 2000.
[22] Williams JG, Cawood MJ. Polym Testing 1990;9:15–26.
[23] Hoff EA, Robinson DW, Willbourn AH. J Polym Sci 1955;18:161–76.
[24] Heijboer J. Physics of non-crystalline solids. Amsterdam: North Holland, 1965. p. 231.
[25] Boyer RF. Polym Engng Sci 1968;8:161–85.
[26] Heijboer J. J Polym Sci Symp C 1968;16:3755–63.
[27] Wellinghoff ST, Baer E. J Appl Polym Sci 1978;22:2025–45.
[28] Nielsen LE. J Macromol Sci-Revs Macromol Chem 1969;C3(1):69–103.
[29] Treloar LRG. The physics of rubber elasticity. London: Oxford, 1958.
[30] Crawford E, Lesser AJ. J Polym Sci: Part B: Polym Phys 1998;36:1371.
[31] Graessley WW. Macromolecules 1975;2:186.
[32] Queslel JP, Mark JE. Adv Polym Sci 1984;65:135.
[33] Langley NR. Macromolecules 1968;1:348.
[34] Fischer M. Adv Polym Sci 1992;100:313.
[35] Mark JA. Physical properties of polymers handbook. New York: American Institute of Physics, 1996.
[36] Butterworth L. PhD Thesis, University of Leeds, UK, 1995.